DOI: 10.1002/chem.200903272

New Fluorinated Rhodamines for Optical Microscopy and Nanoscopy

Gyuzel Yu. Mitronova, Vladimir N. Belov,* Mariano L. Bossi, Christian A. Wurm, Lars Meyer, Rebecca Medda, Gael Moneron, Stefan Bretschneider, Christian Eggeling,* Stefan Jakobs, and Stefan W. Hell*[a]

Abstract: New photostable rhodamine dyes represented by the compounds **1a–r** and **3–5** are proposed as efficient fluorescent markers with unique combination of structural features. Unlike rhodamines with monoalkylated nitrogen atoms, *N*′,*N*-bis(2,2,2-trifluoroethyl) derivatives **1e**, **1i**, **1j**, **3**-H and **5** were found to undergo sulfonation of the xanthene fragment at the positions 4′ and 5′. Two fluorine atoms were introduced into the positions 2′ and 7′ of the 3′,6′-diaminoxanthene fragment in compounds **1a–d**, **1i–l** and **1m–r**. The new rhodamine dyes may be excited with $\lambda = 488$ or 514 nm light; most of them emit light at $\lambda = 512$–554 nm (compounds **1q** and **1r** at $\lambda = 576$ and 589 nm in methanol, respectively) and have high fluorescence quantum yields in solution (up to 98%), relatively long excited-state lifetimes (>3 ns) and are resistant against photobleaching, especially at high laser intensities, as is usually applied in confocal microscopy. Sulfonation of the xanthene fragment with 30% SO_3 in H_2SO_4 is compatible with the secondary amide bond (rhodamine-CON(Me)CH_2CH_2COOH) formed with $MeNHCH_2CH_2COOCH_3$ to providing the sterically unhindered carboxylic group required for further (bio)conjugation reactions. After creating the amino reactive sites, the modified derivatives may be used as fluorescent markers and labels for (bio)molecules in optical microscopy and nanoscopy with very-high light intensities. Further, the new rhodamine dyes are able to pass the plasma membrane of living cells, introducing them as potential labels for recent live-cell-tag approaches. We exemplify the excellent performance of the fluorinated rhodamines in optical microscopy by fluorescence correlation spectroscopy (FCS) and stimulated emission depletion (STED) nanoscopy experiments.

Keywords: dyes/pigments · fluorescence · fluorine · microscopy · rhodamines

Introduction

Fluorescence microscopy is one of the most versatile tools in modern life sciences. Its sensitivity mainly depends on the brightness of the applied fluorescent markers. Photophysical and -chemical parameters, such as a high-absorption cross-section, high fluorescence quantum yield, low degree of triplet or dark-state formation, high photostability, good solubility in water and high labeling capability of, for example, biomolecules determine the usability of a fluorophore.[1] Photostable and bright organic dyes served well in recent advancements of optical microscopy, such as the detection of single molecules[2] or fluorescence nanoscopy.[3] Single-molecule based detection (SMD) technologies, such as fluorescence correlation spectroscopy (FCS)[4] or fluorescence intensity distribution analysis (FIDA) or photon-counting histogram analysis (PCH)[5] may efficiently determine molecular heterogeneities and have even successfully been applied in high-throughput drug discovery,[6] but they require the acquisition of as much fluorescence signal as possible in the shortest time. That is why large laser intensities are often applied in SMD, demanding a new degree of photostability of the dyes in use, as such large intensities promote the population of highly excited electronic states and, consequently, the very efficient photobleaching of the fluorescent dyes.[7] High laser intensities are also required in imaging techniques, such as stimulated depletion emission (STED) nano-

[a] Dr. G. Y. Mitronova, Dr. V. N. Belov, Dr. M. L. Bossi, Dr. C. A. Wurm, Dr. L. Meyer, Dr. R. Medda, Dr. G. Moneron, Dr. S. Bretschneider, Dr. C. Eggeling, Dr. S. Jakobs, Prof. Dr. S. W. Hell
Department of Nano-Biophotonics
Max Planck Institute for Biophysical Chemistry
Am Fassberg 11, 37077 Göttingen (Germany)
Fax: (+49) 551-2012505
E-mail: vbelov@gwdg.de
ceggeli@gwdg.de
shell@gwdg.de

Supporting information for this article is available on the WWW under http://dx.doi.org/10.1002/chem.200903272.

scopy,[3a,d] a fluorescence microscopy technique that has truly surpassed the spatial resolution limit of conventional far-field microscopy given by diffraction.[8] Here, strong additional laser light allows for the spatially-selective inhibition of the marker's fluorescent state by stimulated emission, thereby restricting the remaining fluorescence signal to sub-diffraction sized areas. Although, the additional laser light is not really absorbed by the dye, these large intensities also call for photostable markers with a low degree of dark (triplet) state population.[9]

Further, cellular immunolabeling and microscopy applications, such as multicolor detection and colocalization experiments require a flexible choice of reagents, that is, the availability of the whole gamut of photostable labels. Rhodamine dyes bring along all of the desired photophysical and -chemical characteristics and may serve as a basis for further, versatile improvements. Rhodamines have thus proven advantageous in modern fluorescence microscopy or SMD applications.[10] Here, we present new bright and photostable fluorinated rhodamine dyes based on the structure of Rhodamine 110 (see Scheme 1). The new rhodamines are efficiently excited between $\lambda = 488$ and 515 nm and emit light at around $\lambda = 520$ nm with high fluorescence quantum yields close to one. They have long fluorescence lifetimes of about 4 ns, low triplet yield and feature an extreme photostability, especially at large laser intensities and above all, their water solubility allows an efficient coupling to biomolecules. The STED nanoscopy images with superior spatial resolution over conventional microscopy, single-molecule based FCS measurements and the capability to penetrate into live-cells prove the new rhodamines to be versatile markers for modern microscopy and nanoscopy.

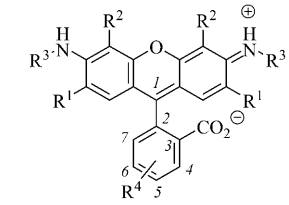

1a: $R^1 = F$, $R^2 = R^3 = R^4 = H$
1b: $R^1 = F$, $R^2 = R^3 = H$, $R^4 = COOH$
1c: $R^1 = F$, $R^2 = SO_3H$, $R^3 = R^4 = H$
1d: $R^1 = F$, $R^2 = SO_3H$, $R^3 = H$, $R^4 = COOH$
1e: $R^1 = R^2 = R^4 = H$, $R^3 = CH_2CF_3$
1f: $R^1 = R^2 = H$, $R^3 = CH_2CF_3$, $R^4 = COOH$
1g: $R^1 = R^4 = H$, $R^2 = SO_3H$, $R^3 = CH_2CF_3$
1h: $R^1 = H$, $R^2 = SO_3H$, $R^3 = CH_2CF_3$, $R^4 = COOH$
1i: $R^1 = F$, $R^2 = R^4 = H$, $R^3 = CH_2CF_3$
1j: $R^1 = F$, $R^2 = H$, $R^3 = CH_2CF_3$, $R^4 = COOH$
1k: $R^1 = F$, $R^2 = SO_3H$, $R^4 = H$, $R^3 = CH_2CF_3$
1l: $R^1 = F$, $R^2 = SO_3H$, $R^3 = CH_2CF_3$, $R^4 = COOH$

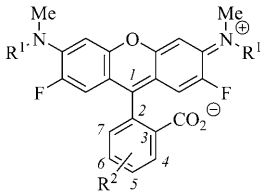

1m: $R^1 = R^2 = H$
1n: $R^1 = H$, $R^2 = COOH$
1o: $R^1 = CH_2CF_3$, $R^2 = H$
1p: $R^1 = CH_2CF_3$, $R^2 = COOH$
1q: R^1= Me, $R^2 = H$
1r: $R^1 = Me$, $R^2 = COOH$

Scheme 1. New fluorinated rhodamines prepared in this study.

Results and Discussion

The route to new fluorinated rhodamines: So far, several classes of the photostable organic substances have been used as scaffolds for the design of improved fluorescent dyes, for example, pyrenes, terrylenes and other condensed polycyclic aromatic compounds, coumarines, rhodols, rhodamines and BODIPY derivatives. Further, attempts to device and improve photostable dyes of other classes, especially emitting in the red-spectral region, are being actively undertaken first of all for the water-soluble terrylenediimides[11] and dicyanomethylene dihydrofuranes.[12] However, not all of the above mentioned dyes can easily be chemically modified and improved. For example, it was rather difficult to modify the BODIPY residue in such a way, that it becomes water soluble.[13] On the contrary, many rhodols or rhodamines may easily be decorated with two sulfonic acid groups simply by sulfonation with SO_3 in H_2SO_4. Sulfonation is known not only to improve solubility in aqueous media, but it also considerably reduces aggregation and quenching of fluorescence in water or aqueous buffers. Introduction of the sulfonic acid residues is known to often increase the photostability and fluorescence quantum yield of a fluorescent dye in solution and after attaching it to a biological macromolecule.[14] In the case of fluorescein, substitution of the aromatic hydrogen atoms at the positions 2′ and 7′ of the xanthene fragment is known to increase photostability, without changing the absorption and emission spectra.[15] The same may be true for rhodamines: fluorination of the xanthene fragment at these positions is very likely to increase the photoresistance of a dye, keeping other spectral properties intact. Surprisingly, no data on 2′,7′-difluorosubstituted rhodamines have been reported in the literature.[16] However, fluorinated rhodol derivatives have been disclosed.[17] Rhodols—3-amino-6′-hydroxyxanthenes—have lower absorption coefficients than the corresponding fluorescein or rhodamine derivative and their fluorescent quantum yields (Φ_{fl}) are lower than these of fluorescein derivatives or rhodamines.[18] Substituted rhodols are used as sensor for metal ions, but not as bright and photostable fluorescent labels in microscopy and optical imaging. Another new and important feature of the rhodamines introduced in the present study is a combination of the two 2,2,2-trifluoroethyl amino groups at the positions 3′ and 6′ with the two sulfonic acid residues at the positions 4′ and 5′ of the xanthene ring. In 1989 and 1991 a very limited number of *N,N*′-bis(2,2,2-trifluoroethyl)-3′,6′-diaminoxanthenes have been already disclosed as photostable analogues of Rhodamine 6G but these patents[19] have very narrow claims and do not deal with any of the compounds presented here. We chose the 2,2,2-trifluoroethyl residue as a substituent for the amino group for the following reasons.[3r] In some respects, it behaves like a hydrogen atom. For example, 2,2,2-trifluoropropionic acid (CF_3CH_2COOH) is as strong as formic acid (HCOOH). This means that the electronic inductive effect of the CF_3CH_2-group is equal to the inductive effect of the hydrogen atom. Fluorination is known to increase the lipo-

philicity and reduce the solubility in water. Sulfonation compensates this effect and restores the hydrophilic properties of dyes, providing a fairly good solubility in water. Sulfonation is known to shift very slightly both the absorption and the emission bands to the blue (up to $\approx$5 nm),[3p] but it does not alter the spectral properties considerably. We found that the presence of one CH_2CF_3 group at the nitrogen atom in rhodamine does not inhibit the sulfonation with SO_3 in H_2SO_4. On the other hand, the $NHCH_2CF_3$-groups in the derivatives of amino acid are resistant to acylation (in the presence of "normal" primary amines).[20] Thus, this residue provides a sufficient chemical protection for the amino group and it also reduces the number of NH atoms prone to photobleaching reactions.

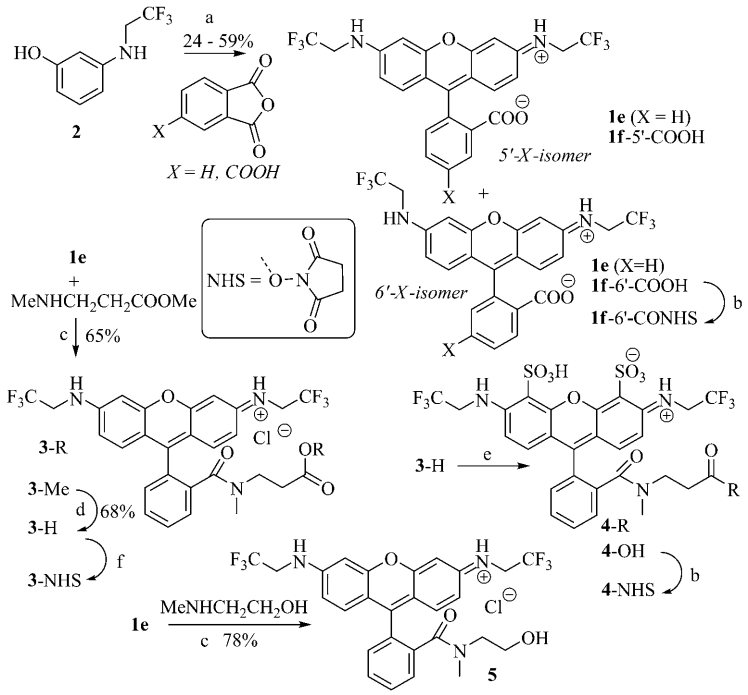

Scheme 2. Synthesis of *N,N′*-bis(2,2,2-trifluoroethyl)rhodamines **1e** and **1f**, amides **3**-R and **5**, sulfonated amide **4**-OH, as well as NHS-esters **1f**-6′-CONHS and **4**-NHS: a) 160 °C, 3 h, then second half of **2**, 85 % aq. H_3PO_4, 160 °C, 3 h; b) *N*-hydroxysuccinimide, *O*-(7-azabenzotriazol-1-yl)-*N,N,N′,N′*-tetramethyluronium·PF_6^- (HATU), DMF, RT, overnight; c) $POCl_3$, 1,2-dichloroethane, reflux, 4 h; then a secondary amine, Et_3N, MeCN, RT, 20 h; d) 1 M aq. NaOH, MeOH, THF, 0 °C→RT, 2 h; e) 30 % SO_3 in H_2SO_4, 0 °C, 2–3 days; f) *N,N,N′,N′*-tetramethyl-*O*-(*N*-succinimidyl)uranium·BF_4^- (TSTU), Et_3N, DMF, RT, 24 h.

Rhodamine 110 (Rh110) is a convenient reference and starting compound for the introduction of the structural modifications mentioned above. Rh110 is a well known laser dye,[21] with an absorption maximum at $\lambda = 496$ nm and emission at $\lambda = 520$ nm (in water). It exhibits a bright-green fluorescence ($\Phi_{fl} = 0.92$ in basic ethanol).[22] For the reasons mentioned above, all derivatives of Rh110 depicted in Scheme 1 (compounds **1a–l**) are expected to have the same absorption and emission spectra as the parent dye.

Synthesis of the fluorinated and sulfonated rhodaminic dyes and their NHS esters: Synthetic routes to the new fluorinated rhodamines are given in Schemes 2–6. The synthesis and amidation of rhodamine **1e** have been already described.[3r] Condensation of aminophenol **2** with 4-carboxyphthalic anhydride led to the mixture of 5′- and 6′-carboxyrhodamines **1f**-5′/6′-COOH (Scheme 2).

By the repeated recrystallization of this mixture from aqueous *i*PrOH, the nearly pure regioisomer **1f**-5′-COOH may be isolated (with less than 4 % of **1f**-6′-COOH). Evaporation of the combined mother liquids followed by reversed-phase chromatography with MeOH/H_2O mixture (1:4) gave the second pure diastereomer (**1f**-6′-COOH). Derivatisation of the monocarboxy rhodamine **1f** is necessary for bioconjugation.[23] For that, rhodamine **1f** was converted into the corresponding acid chloride and the latter reacted with methyl 3-[(*N*-methyl)amino]propionate or 2-[*N*-(methylamino)]ethanol (Scheme 2). Saponification of the methyl ester **3**-Me smoothly gave the acid **3**-H, which was transformed into the NHS-ester **3**-NHS. *N,N′*-Disuccinimidylcarbonate in the presence of a base transforms alcohol **5** into the corresponding NHS-carbonate. Rhodamines with two carboxylic groups (e.g., **1f**-6′-COOH) react with one equivalent of *N*-hydroxysuccinimide and *O*-(7-azabenzotriazol-1-yl)-*N,N,N′,N′*-tetramethyluronium·PF_6^- (HATU), or with 1 equivalent of *N,N,N′,N′*-tetramethyl-*O*-(*N*-succinimidyl)uronium tetrafluoroborate (TSTU) in the presence of a base and yield mono NHS-esters with the sterically less hindered carboxylic group activated by the formation of an ester with a good leaving group (e.g., **1f**-6′-CONHS).

We observed that the secondary amide group in rhodamines is quite stable under sulfonation conditions (30 % SO_3 in H_2SO_4, 0 °C) for several days. Thus, sulfonation of the acid **3**-H affords disulfonic acid **4**-OH with an intact amide bond (Scheme 2). It was found to be much easier to obtain the corresponding rhodamine amide first and then to sulfonate it, than to perform the reversed procedure, which requires two tedious reversed-phase chromatographic separations instead of one and in which the yield at the amidation step is lower.

Commercially available 2-fluoro-5-nitroaniline (**7**) was used as a starting material for the synthesis of other fluorinated rhodamines (Scheme 3). It was transformed to *N*-methyl- (**8**-NO_2-Me) and *N,N*-dimethylaniline **6**-NO_2 and then nitro groups in these compounds and in the intermedi-

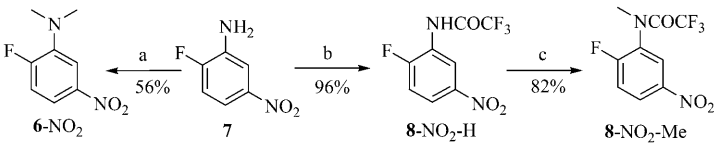

Scheme 3. Preparation of 2-fluoro-5-nitroanilines **6**-NO_2 and **8**-NO_2: a) 35% aq. H_2CO, $NaBH_4$, THF, 3 M aq. H_2SO_4, RT; b) $(CF_3CO)_2O$, CH_2Cl_2, Et_3N, 0 °C→RT, overnight; c) MeI, K_2CO_3, DMF, 90 °C, 24 h.

ate **8**-NO_2-H were reduced (Schemes 4 and 5). The next important step included the diazotation of the anilines **8**-NH_2-R (Scheme 4) and **6**-NH_2 (Scheme 5) followed by the transformation of diazonium salts into phenols **8**-OH-R and **6**-OH under very mild conditions.[24] Compound **6**-OH was directly used in the synthesis of rhodamine **13**-Me-Me-H (**1q**) with one carboxylic acid group and the mixture of regioisomers **13**/**14**-Me-Me-COOH (**1r**) with two carboxylic acid groups (Scheme 6).

N-Trifluoroacetylated *m*-aminophenols **8**-OH-R (Schemes 4 and 5) were the key intermediates for the following transformations. They were either reduced to 3-hydroxy-*N*-(2,2,2-trifluoroethyl)anilines **10**-R (Scheme 4), or deprotected to anilines **12**-R^1 (Scheme 5). *m*-Aminophenols **10**-R and **12**-R^1 were condensed with phthalic or trimellitic anhydrides and rhodamines **9**-H-H (**1i**), **9**/**11**-H-COOH (**1j**), 9-Me-H (**1o**), **9**/**11**-Me-COOH (**1p**), **13**-H-H-H (**1a**), **13**/**14**-H-H-COOH (**1b**), **13**-Me-H-H (**1m**) and **13**/**14**-Me-H-COOH (**1n**) were obtained. All rhodamines in Schemes 4 and 5 were obtained in the course of the condensation reaction in the presence of fused anhydrous $ZnCl_2$ and isolated from the reaction mixtures by column chromatography on silica gel. Unoptimized yields were found to be moderate.

The stepwize condensation reaction exemplified in Scheme 2 can be applied to two various *m*-hydroxyanilines chosen from the set of compounds **2**, **10**-R (Scheme 4) and **12**-R (Scheme 5). This approach may enable the synthesis of the unsymmetrical rhodamines (3′,6′-diaminoxanthenes) with various combinations of the substituents.

The feasible sulfonation reactions are given in Scheme 6. As in the case of compound **3**-H (Scheme 2), *N*-(2,2,2-trifluoroethyl) substituents did not prevent the sulfonation and the corresponding disulfonic acids **1k–l** and **1h**-5′-COOH were obtained (Scheme 6). The presence of methyl groups at the nitrogen atoms in rhodamines inhibited the sulfonation reactions completely, though the steric hindrance caused by methyl groups is supposed to be even less than that of 2,2,2-trifluoroethyl groups. Probably, *N*-alkylamino groups increase the basicity of nitrogen atoms (compared with unsubstituted or mono 2,2,2-trifluoroethyl substituted ones) and an excess of SO_3 in H_2SO_4 forms a very stable complex only with mono *N*-alkylamino groups, inhibiting the aromatic S_E-reaction. Sulfonation was found to be always regioselective: only C-4′ an C-5′ atoms were sulfonated. This fact may be explained by the lower localization energy for the position 1 than for the position 2 in

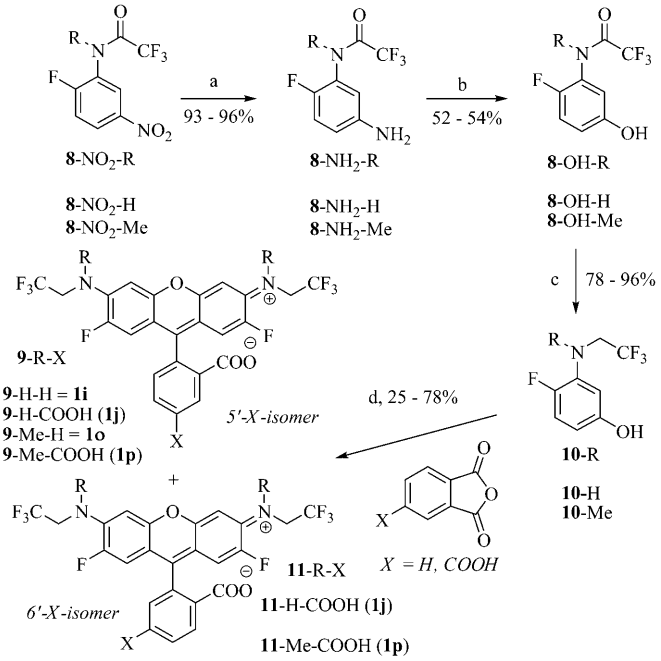

Scheme 4. Synthesis of 2,7-difluoro-*N*,*N*′-bis(2,2,2-trifluoroethyl)rhodamines **9** and **11** (**1i–j**, **1o–p**): a) 10% Pd/C, H_2, EtOAc, RT, 7 h; b) aq. $NaNO_2$, 35% aq. H_2SO_4, 0 °C, then aq. $Cu(NO_3)_2{\cdot}3H_2O$, Cu_2O, RT; c) 1 M BH_3·THF, THF, 0→90 °C, 24 h; d) fused $ZnCl_2$, 180–200 °C, 3–4 h.

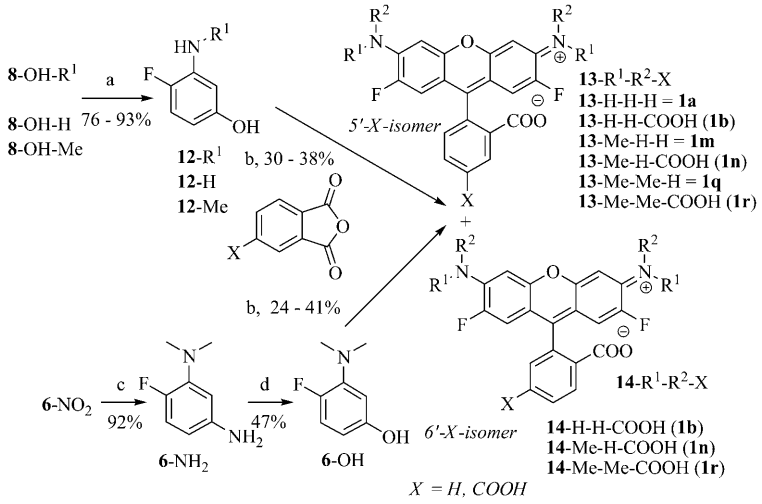

Scheme 5. Synthesis of 2,7-difluororhodamines **13** and **14** (**1a–b**, **1m–n**, **1q–r**): a) 30% aq. NaOH, MeOH, 90 °C, 24 h; b) fused $ZnCl_2$, 180–200 °C, 3–4 h; c) 10% Pd/C, H_2, EtOAc, RT, 7 h; d) aq. $NaNO_2$, 35% aq. H_2SO_4, 0 °C, then aq. $Cu(NO_3)_2{\cdot}3H_2O$, Cu_2O, RT.

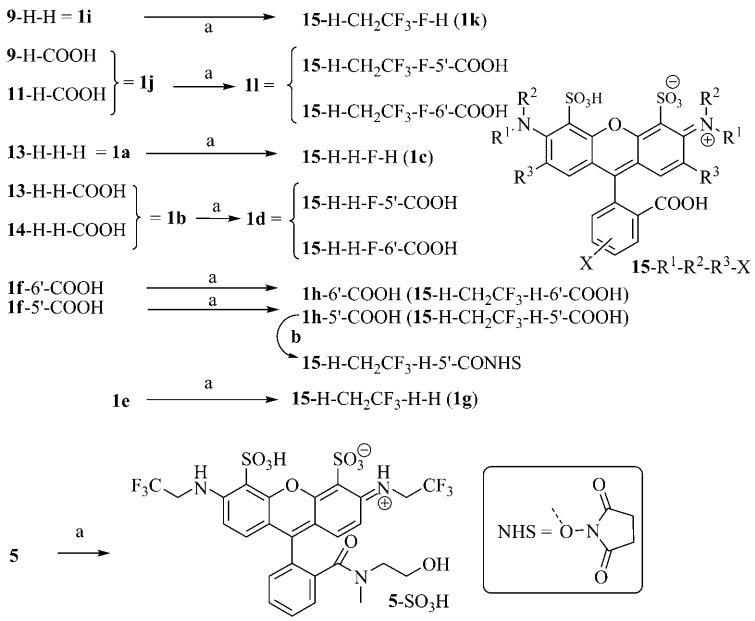

Scheme 6. Sulfonation of *N*,*N*′-bis(2,2,2-trifluoroethyl)rhodamines **1k**–**l**, **1f**-5′-COOH, as well as *N*,*N*′-unsubstituted 2,7-difluororhodamines **1j**, **1a**–**b** and alcohol **5**: a) 30% SO_3 in H_2SO_4, 0°C, 2–3 days; b) *N*-hydroxysuccinimide, HATU, DMF, RT, overnight.

9,10-disubstituted anthracenes (if the reaction is thermodynamically controlled).

Activation of the sterically available carboxylic group in rhodamines may be achieved by the formation of the active esters (e.g., NHS-esters **1f**-6′-CONHS, **3**-NHS and **4**-NHS in Scheme 2). Together with compound **15**-H-CH_2CF_3-H-5′-CONHS in Scheme 6, these esters were used in bioconjugation reactions described in one of the following sections.

Spectral properties: Most of dyes of the present study are highly fluorescent and all of them are photostable compounds in water, aqueous buffers, alcohols and typical mounting media used in standard fluorescence microscopy techniques, such as polyvinyl alcohol (PVA), or its mixtures with water and glycerol. The majority of the compounds form colored and fluorescent solutions in a wide pH range from pH 1 to 12. They have absorption maxima between $\lambda =$ 480 and 515 nm with high extinction coefficients of up to $\varepsilon \approx 9\times10^4\,\text{M}^{-1}\text{cm}^{-1}$ and emit in the $\lambda = 510$–535 nm region with high emission efficiencies, that is, fluorescence quantum yields of up to 0.95. Their solutions are yellow or light orange in daylight and have a yellow-greenish or yellow emission when excited with blue light. Compounds **9**-Me-H (**1o**), **13**-Me-Me-H (**1q**) and **13/14**-Me-Me-COOH (**1r**) absorb and emit at $\lambda = 525$–560 nm and 555–580 nm, respectively. Their solutions have a pink or red color. An example of the absorption and emission spectra for compound **13**-H-H-H (**1a**) is shown in Figure 1.

In acidic solutions ($\text{pH} \le 5$), a small bathochromic shift in absorption and emission maxima (typical 5 nm) was commonly observed (Figure 1). It may be caused by the protonation of the benzoic acid moiety. However, none or only minor changes in the spectra are observed in the biologically relevant pH region of 6–9. Further, most of the fluorinated rhodamines presented here have fluorescence lifetimes of 3–4 nanoseconds that are typical for rhodamines. The spectral properties, extinction coefficients and fluorescence lifetime values of the fluorinated rhodamines are summarized in Table 1.

A strong absorption maximum at $\lambda = 290$–300 nm, characteristic for the compounds **1o** and **1p**, indicates the presence of closed non-fluorescent forms with a spirolactone fragment. For example, compound **1o** gives colorless solutions in methanol, water and neutral buffers. In acidic solutions,

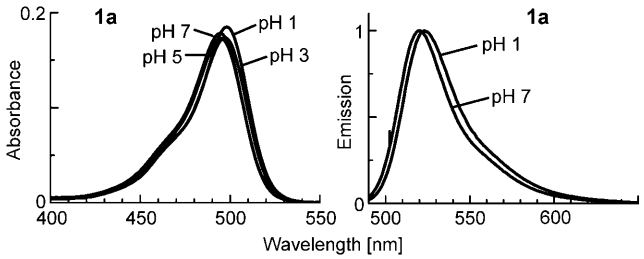

Figure 1. Spectral properties. Absorption and fluorescence emission spectra of compound **13**-H-H-H (**1a**) in the pH range 1–7.

compound **1o** exists in an open acidic form with relatively low fluorescence efficiency. The acid-base equilibrium (see Scheme S1 in the Supporting Information), which is responsible for the absence of color and fluorescence of compound **1o** in neutral solutions, was not observed for the other compounds.

Photostability at low laser intensities: The photostability of a fluorophore determines the observation time of fluorescence microscopy experiments and is mainly characterized by the chemical "fragility" of the excited states.[1,25] As mentioned, the photostability of rhodamines depends on the substitution pattern in the 3′,6′-diaminoxanthene fragment. Comparison of Rhodamine 6G (with disubstituted nitrogen groups), Tetramethyl rhodamine (TMR; with trisubstituted nitrogen atoms) and methyl ester of Rhodamine 110 (with monosubstituted nitrogen groups) showed that at low light intensities (up to $10^3\,\text{W cm}^{-2}$) TMR was the most stable dye. Photobleaching quantum yields in water were found to be 12, 3.3 and 6.6×10^{-7}, respectively.[7] It is interesting that

Table 1. Spectral properties of the fluorinated rhodamines.

Compound	Absorption		Emission		
	λ_{max} [nm]	ε [$\times 10^{-4}$ M^{-1}cm^{-1}]	λ_{max} [nm]	Φ_{fl}[a]	τ_{fl} [ns][a]
1a (**13**-H-H-H)	494,[a] 498[b]	4.1[b]	520,[a] 522[b]	0.87	3.9
1b (**13/14**-H-H-COOH)	496,[a] 498[b]	5.0[b]	522,[a] 523[b]	0.92	4.0
1c (**15**-H-H-F-H)	488,[a] 498[b]	4.2[b]	512,[a] 514[b]	0.89	4.0
1d (**15**-H-H-F-COOH)	490,[a] 502[b]	3.2[b]	514,[a] 517[b]	0.97	4.1
1e	499[a]	8.1[a]	522[a]	0.88	3.9
1f-5′-COOH	501,[a] 500[b]	8.5[a]	525,[a] 524[b]	0.95	4.1
1f-6′-COOH	501,[a] 497[b]	8.8[a]	523,[a] 522[b]	0.93	–
1g (**15**-H-CH_2CF_3-H-H)	499,[a] 507[b]	8.7[b]	520,[a] 524[b]	0.88	3.8
1h-5′-COOH (**15**-H-CH_2CF_3-5′-COOH)	501,[a] 511[b]	8.6[b]	524,[a] 524[b]	0.96	3.9
1i (**9**-H-H)	494,[a] 500,[b] (292)[2b]	4.1[b]	521,[a] 519[b]	1.00	3.8
1j (**9/11**-H-COOH)	496,[a] 498[b]	5.3[a]	522,[a] 520[b]	0.89	3.8
1k (**15**-H-CH_2CF_3-F-H)	506[a]	5.4[a]	531[a]	0.66	3.2
1L (**15**-H-CH_2CF_3-F-COOH)	509,[a] 517[b]	4.2[b]	533,[a] 541[b]	0.86	3.3
1m (**13**-Me-H-H)	513,[a] 511[b]	5.6[b]	539,[a] 537[b]	0.87	4.0
1n (**13/14**-Me-H-COOH)	515,[a] 515[b]	5.6[b]	543,[a] 538[b]	0.86	4.1
1o (**9**-Me-H)	(528)[1a] (300)[2b]	(3.2)[1a]	(557)[1a]	(0.20)[1]	(1.2)[1]
1p (**9/11**-Me-COOH)	(523),[a+b] (291)[2b]	–	–	–	–
1q (**13**-Me-Me-H)	554,[a] 546[b]	5.0[a]	586,[a] 576[b]	0.02	3.3
1r (**13/14**-Me-Me-COOH)	525,[a] 558[a+b]	3.1[a]	554,[a] 589[b]	0.28	1.6
3-Me	512[b]	8.7[b]	534[b]	–	–
3-H	510,[a] 512[b]	5.7[a]	531,[a] 534[b]	0.86	4.2
4-OH	512,[a] 517[b]	7.4[b]	530,[a] 536[b]	0.86	4.1
5	510,[a] 512[b]	7.1[b]	531,[a] 534[b]	0.86	4.2
5-SO_3H	512[a]	5.2[a]	530[a]	0.86	4.1

[a] In an aqueous buffer at pH 7. [b] In methanol. [a+b] Mixture. [1] Values measured at pH 1. [2] Value for the closed form.

under these conditions, methyl ester of Rh110 bleached slower than Rhodamine 6G, though the degree of substitution at the nitrogen atoms of latter compound is higher. This fact may be explained by the presence of two methyl groups at the positions 2′ and 7′ of Rhodamine 6G: they block the carbon atoms of the xanthene heterocycle, but, at the same time, these methyl groups may give rise to the relative stable benzylic radicals—good carriers in the chain radical processes during photobleaching. Another possible explanation relies on the relative polarities of the dyes: Rhodamine 6G is much less polar and poorly solvated in water than the methyl ester of Rh110.

Further, photobleaching of rhodamines involves energy-rich radical intermediates (which are electron-deficient, as they lack one electron of the stable electron octet).[26] Therefore, it is quite reasonable to assume that the rate-limiting step of the bleaching reaction also involves radical species as intermediates. According to the Hammond's postulate, the geometry of a transition state of an endothermic reaction leading to a radical intermediate is better approximated by the geometry of a radical than by the geometry of the initial substance (reactant). This means that any effects (de)stabilizing the intermediate radical species will (de)stabilize the transition state, as well. The fluorine atoms with their strong negative inductive effect ($-I$-effect) not only substitute hydrogen atoms and reduce the probability of their abstraction in the course of bleaching reactions, but also destabilize radical centers. In this case, the $-I$-effect of fluorine atoms in the intermediate radicals should increase the activation energy of their formation (compared with the similar reaction of a non-fluorinated substrate) and slow-down photobleaching.

Our new fluorinated rhodamines display an outstanding photostability when irradiated for a prolonged time with low laser intensities ($<$ kW cm^{-2}). Figure 2 shows the emission intensity of the stirred solutions with micromolar concentrations of some exemplary compounds, when irradiated with $\lambda = 488$ nm light in a 1 cm-path quartz cuvette, at an intensity of 3 W cm^{-2}. The initial absorption at the irradiation wavelength was the same for all solutions. The compounds are far more stable than the common dyes excitable at $\lambda = 488$ nm, such as Fluoresceine and Oregon Green® 488 and have similar or even better performance than Rhodamine Green or Alexa Fluor 488. For example, aqueous solutions of compounds **1g**, **4**-OH and **1h** can be irradiated for several hours with the $\lambda = 488$ nm line of an Argon laser without any significant changes in their emission. After two hours of irradiation, compounds **1e** and **1f** retain more than 50% of the initial emission intensity and compound **3**-H has about 90% of the initial signal left.

Performance at high laser intensities: Maximizing the sensitivity of fluorescence microscopy often requires maximizing the fluorescence rate, that is, the fluorescence emission

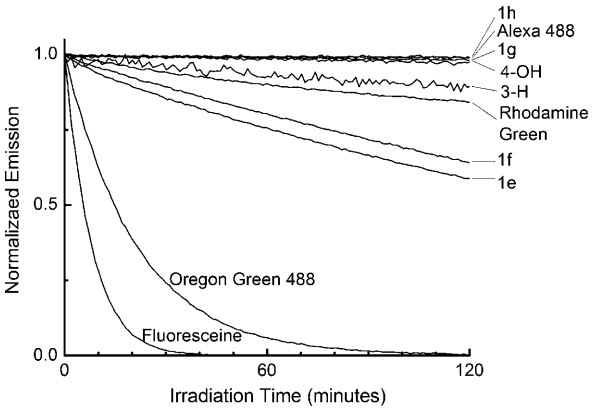

Figure 2. Photostability at low excitation intensities. Decrease of fluorescence signal over time due to photobleaching with 3 W cm^{-2} of $\lambda =$ 488 nm laser light of selected new rhodamines (**1e**–**h**, **3**-H and **4**-OH) and, for comparison, of some commercially available fluorescent dyes with the similar spectral properties (Alexa Fluor 488, Rhodamine Green, Oregon Green 488 and Fluorescein) in aqueous solutions. At low laser intensities, some of the new rhodamines allow for observation times of several hours, superior over some other commercially available dyes.

within a certain time span, which is usually approached by applying large excitation intensities of laser light. For example, in common microscopy, such as confocal or single-molecule based techniques, fluorescent markers are subject to excitation intensities much higher than those mentioned above, and are in the range of a few kW cm^{-2}. The comparative photostabilities presented in Figure 2 may be incorrect under these irradiation conditions, as new photobleaching pathways open up. At high laser intensities, the population of long-lived dark (triplet) states, as well as higher excited electronic states, is much more pronounced.[7,27] These states, on one hand, temporally dislodge the dye from the excitation-emission cycle, thus leading to a loss in brightness. On the other hand, they are usually much more reactive, thus introducing much more profound photobleaching.[7,28] For example, in aqueous solution, higher excited electronic states couple quite efficiently with highly-reactive radical states.[7,29]

We applied fluorescence correlation spectroscopy (FCS)[4] to get further insights on the triplet-state population and photobleaching of the new rhodamines at large excitation intensities.[7,26a,30] Figure 3 shows correlation data of compound **1h** and for comparison of Rh110 in aqueous solution at relatively low (115 kW cm^{-2}) and at very large intensities (2 MW cm^{-2}) of $\lambda = 488$ nm laser light. On one hand, the quality of the correlation data depicts that our compounds perform equally well in single-molecule based experiments, such as FCS, like the well-established dye Rh110. On the other hand, the curves are characterized by two decays. The first one in the µs time range is given by population and depopulation of the triplet state. The decay time at low intensities characterizes the triplet-state lifetime, whereas the amplitude reveals the relative triplet population.[30a] No significant difference in triplet lifetime and population is observed

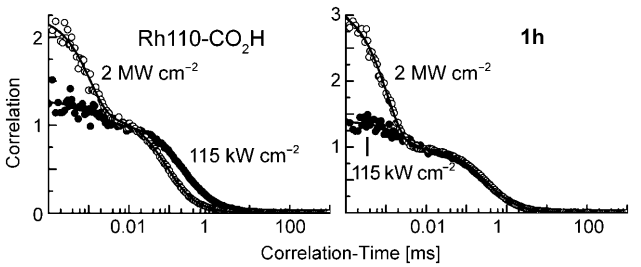

Figure 3. Photostability at high laser intensities. FCS curves obtained from Rh110-CO_2H (left) and compound **1h** (B) in aqueous solution at relatively low (●; 0.1 MW cm^{-2}) and high (○; 2 MW cm^{-2}) excitation intensity (dots: experimental data; lines: best fits). The new rhodamine **1h** shows about the same triplet buildup (decay in µs time range) but much less photobleaching (smaller shift of ms decay to shorter correlation times at larger laser intensities) than Rh110.

between compound **1h** and Rh110. The second decay of the correlation curve in the ms time range characterizes the observation time of the fluorophore, which is usually given by the diffusion time through the laser focus. However, at large laser intensities, photobleaching may dominate the observation time, thus resulting in a shortening of this decay.[7,30b] The increased photostability of compound **1h** becomes obvious.

Fitting of the FCS data resulted in values of the intersystem crossing rate k_{isc}, of the triplet de-excitation rate constant k_T (inverse triplet lifetime τ_T) and of the effective photobleaching cross-section σ_{bl} from higher excited electronic states (see the Supporting Information).[7,26a,30b,31] The lower k_{isc}, k_T and σ_{bl}, the better is the performance of the dye at high laser intensities, that is, the population of the dark triplet state is lower and the photobleaching reactions from higher excited electronic states are less probable. Table 2 depicts the values of k_{isc}, k_T and σ_{bl} of the new rhodamine compounds and, for comparison, of the commercial rhodamines, Rh110 and Alexa Fluor 488. The values confirm that triplet population of the new compounds is comparable to other rhodamines, but photobleaching is efficiently reduced. Note that sulfonation of compound **1f** leads to an improved photostability of compound **1h**.

Table 2. Photostabilities and triplet parameters of the fluorinated rhodamines in an aqueous buffer at pH 7 at large laser intensities.

Compound	Triplet parameters		Photobleaching
	k_{isc} [10^6 s^{-1}][a]	k_T [10^5 s^{-1}][b]	σ_{bl} [10^{-21} cm^2][c]
Rh110	0.8	3	5
Alexa 488	0.7	1.5	2
1f-5′-COOH	0.9	5	1.5
1h-5′-COOH	1	2	0.4
5	1.5	5	0.9
5-SO_3H	2	2.5	0.45

[a] Intersystem crossing rate. [b] Triplet de-excitation rate (inverse triplet lifetime). [c] Effective photobleaching cross-section; all parameters determined by FCS with standard deviations of about 10–20 %.

Clearly, the new rhodamines are advantageous in fluorescence microscopy, both for long observation times at low laser intensities and for maximum brightness and photostability at high laser intensities, that is, under conditions, such as single-molecule based experiments for which the maximum number of photons per time is crucial.

Labeling characteristics: The amino reactive derivatives of the dyes presented here can easily be attached to antibodies (AB) or other bio-molecules in the course of the standard labeling and immunostaining procedures. The labeling of the AB with a reactive (fluorescent) dye involves the dissolution of both components (e.g., in phosphate buffer-saline [PBS] at pH $\approx$8.5) followed by incubation for 1–2 h at room temperature. For conjugation, a 15–20-fold molar excess of a dye dissolved in anhydrous DMF is used. Poor solubility of a dye in aqueous buffers may result in precipitation and low labeling efficiency (low average number of dye molecules per AB), or also some unspecific binding may occur. Another problem, which may arise, is a decrease in the fluorescence quantum yield of the dye-AB adducts. Lipophilic fluorescent dyes are often less bright in polar environments or after binding with proteins. The studied dyes are suitable for conjugation with commercial ABs, yielding highly fluorescent adducts with only minor alterations of the spectral properties. For instance, the absorption and emission spectra of the dye **1h** and related adduct with an AB are shown in Figure 4.

The spectra are very similar, except for the strong absorption band observed for the **1h**-AB conjugate at $\lambda = 280$ nm, which is typical for proteins. Moreover, the dye retained about 75% of its emission efficiency after coupling with the AB.

From the Figure 4, an average labeling efficiency of 4.6 molecules of the fluorescent dye **1h** per antibody is calculated. For Immunoglobulin G, the optimal labeling with rhodamines is achieved with 3–7 residues of a dye attached to one molecule of an AB. The immunostained samples of the AB labeled with fluorinated rhodamines were very bright and stable and gave excellent images in standard fluorescence microscopy and nanoscopy. Examples of these results are given in the next sections.

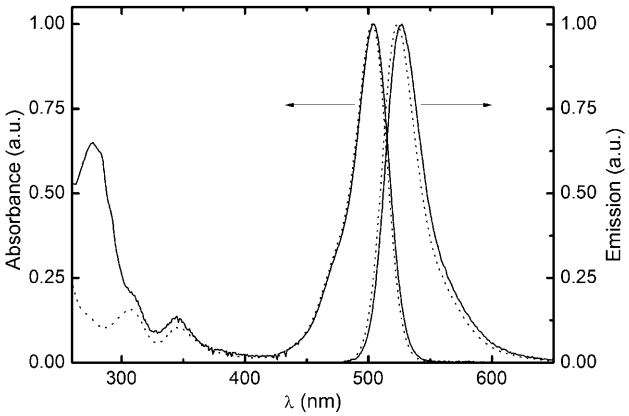

Figure 4. Spectral properties after bioconjugation: Normalized absorption and emission spectra of compound **1h** (-----) and its conjugate with antibodies (——) in PBS solution. No significant shift of the spectra is observed after bioconjugation.

STED nanoscopy: switch-off characteristics: The new fluorinated rhodamines are excellent markers for STED nanoscopy. The additional laser light produced by STED nanoscopy is used to spatially and selectively depopulate the marker's fluorescent state by stimulated emission, thereby restricting the fluorescence emission to sub-diffraction sized areas.[3a,8] An important prerequisite is that strong intensities of the STED laser are applied to saturate the switch-off transition. Although not really absorbing the additional light, the dye has to withstand large intensities without being photobleached too fast. Low saturation intensities, that is, low STED intensities at which 50% of the fluorescence is switched off are favorable, since, in this case, lower laser intensities are required for the same degree of saturation. Figure 5 shows the relative fluorescence switch-off with increasing focal peak intensity of the STED light. Figure 5A and B show data of the dyes in spin-coated PVA layers with 250 kHz pulsed irradiation, whereas Figure 5C shows data of the dyes embedded in mowiol with continuous-wave (CW) light. Excitation was performed at $\lambda = 488$ nm, whereas STED wavelengths were tuned to $\lambda \approx 600$ nm in the pulsed mode and $\lambda = 592$ nm in the CW case. In all cases, the new com-

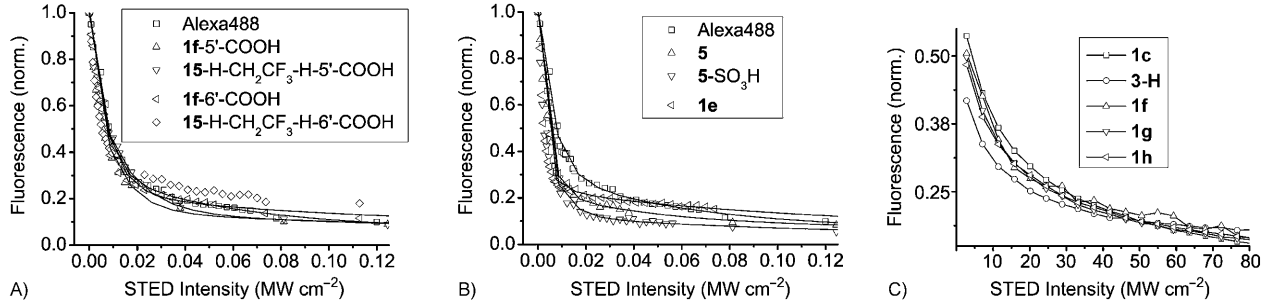

Figure 5. STED nanoscopy and fluorescence switch-off characteristics. Relative fluorescence switch-off with increasing intensity of the STED light for rhodamines in spin-coated PVA layers with 250 kHz pulsed irradiation (A,B) and embedded in mowiol with CW light (C). The new compounds show excellent switch-off characteristics by the STED light with a large saturation degree and low saturation intensities.

pounds showed excellent switch-off characteristics by the STED light with a large saturation degree and time-averaged saturation intensities of ≈1–5 kW cm^{-2} in the 250 kHz case, which are very common values (see for example Alexa 488 in Figure 5A).[9b] In the case of CW excitation, much larger average STED intensities (≈3 MW cm^{-2}) are necessary to achieve the same switch-off efficiency as in the 250 kHz case, which is in line with the theoretically expected increase in saturation intensity $1/(\ln 2 \cdot f \cdot \tau_{fl}) \approx 1450$ (with fluorescence lifetime $\tau_{fl} \approx 4$ ns and pulse repetition rate $f =$ 250 kHz).[32] The photobleaching was found to be low enough to allow accurate recording of these switch-off data, which are as expected from the low photobleaching yields at high-excitation intensities (compare Table 2).

For comparison of the STED images with the corresponding conventional confocal images of cellular samples immunostained with our compounds, see Figure 6: Microtubulin of PtK2 cells labeled with compound **1f** (Figure 6A), vimentin of PtK2 cells labeled with compound **1h** (Figure 6B) and doublecortin of redifferentiated human neuroblastoma cells SH-SY5Y labeled with compound **15** (Figure 6C). Images Figure 6A and B were recorded with CW irradiation (STED intensity 80 MW cm^{-2} at $\lambda = 592$ nm), whereas those of Figure 6C were recorded with 250 kHz pulsed irradiation (with time-averaged STED intensity of ≈100 kW cm^{-2} at $\lambda \approx 600$ nm). In all cases, the images were of high quality with respect to brightness and signal-to-background ratio. Note that the dye **1f** is *not* a sulfonated rhodamine derivative. Nevertheless, it neither produced any background, nor any observable aggregation. Further, the spatial resolution of the STED images was significantly improved over that of the confocal counterparts, allowing an improved disclosure of the structural details.

Labeling of lipids: The use of fluorescent lipid analogues for the study of membrane organization helps to get detailed insight into cellular processes and most importantly into the role of lipid dynamics and the formation of lipid nanodomains or "rafts".[33] Small organic fluorophores as markers are preferable to minimize the influence of the label on the dynamics of the small lipid molecules. Using a combination of STED and FCS, we have previously shown detailed insight of nanoscale dynamics of small organic dye labeled lipids in the plasma membrane of living cells, depicting transient and cholesterol assisted molecular complexes.[34] The new fluorinated rhodamines can also be successfully attached to lipids. For example, the hydrophilic and water-soluble dye **1h**-5′-COOH (or as the NHS ester **15**-H-CH_2CF_3-H-5′-CONHS) was successfully used for labeling of the polar carbohydrate domain in the derivative of the natural glycosphingolipid GM1 (Scheme 7).[3q]

The starting compound **16** was obtained from the natural GM1 ganglioside ($R^1 = CH_3CO$, $R^2 = CH_3(CH_2)_{16}CO$) by alkaline hydrolysis, in the course of which the acetyl group in the neuraminic acid residue and the stearic acid fragment had been cleaved off. Owing to the higher activity of the primary amino group in the sphingosine moiety, diamine **16** can be selectively labeled by two various markers. The first

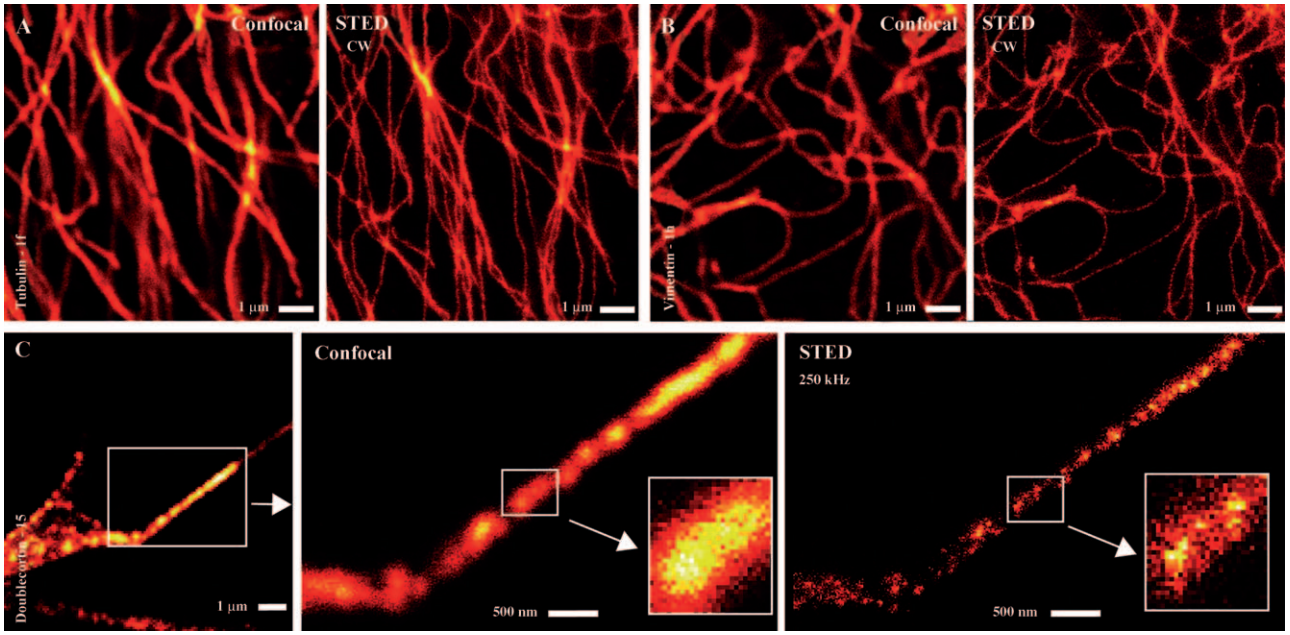

Figure 6. STED nanoscopy and imaging. STED and according conventional confocal images of immunostained cellular samples: A) Microtubules of PtK2 cells labeled with compound **1f**, B) vimentin of PtK2 cells labeled with compound **1h**, and C) doublecortin of redifferentiated human neuroblastoma cells SH-SY5Y labeled with the compound **15**. Images A) and B) were recorded with CW irradiation (STED intensity 80 MW cm^{-2} at $\lambda = 592$ nm), whereas those of C) were recorded with 250 kHz pulsed irradiation (STED intensity 2.1 GW cm^{-2} at $\lambda \approx 600$ nm). In all cases, the images were of high quality with respect to brightness and signal-to-background ratio, that is, the immunolabeling is excellent and the spatial resolution of the STED images is significantly improved over the confocal counterparts, allowing for an improved disclosure of structural details.

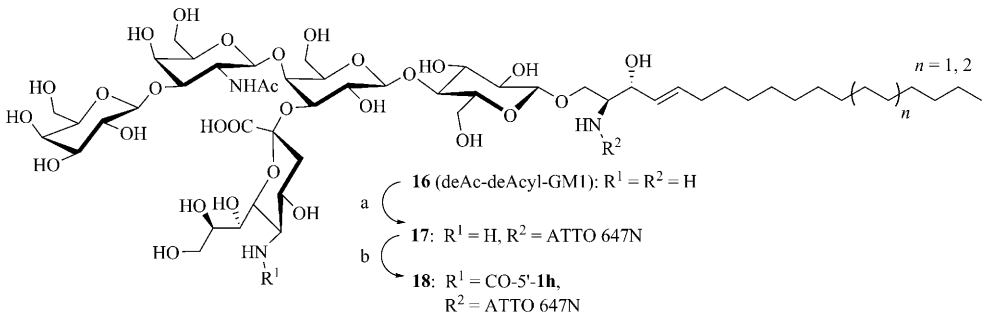

Scheme 7. Derivatives of the natural GM1 ganglioside with fluorescent labels: a) ATTO 647N NHS ester, DMSO, NEt_3, RT, 24 h; b) **1h**-5′-COOH, DMSO, HATU, NEt_3, RT, 24 h (or **15**-H-CH_2CF_3-H-5′-CONHS in DMSO at RT).

one has to be preferably lipophilic, to mimic the natural stearic acid fragment. Therefore, the unpolar fluorescent dye (ATTO 647N) was used at the first step. The second marker has to be hydrophilic, as it labels the polar carbohydrate domain. Compound **18** was successfully used in two-color FCS experiments).[3q]

Studies on the intracellular availability of the new fluorescent dyes: Microscopic imaging of protein dynamics and distribution in living cells is one of the most important tasks in cell biology. For imaging of specifically labeled proteins in living cells, the genetically created chimeric proteins consisting of a host protein and a reporter protein are used in most cases. In addition to the available fluorescent fusion proteins, several strategies, such as SNAP-, CLIP- or Halo-tags were established over the last years to label proteins in living cells specifically with organic fluorophores.[35] Modified cellular enzymes are applicable for covalent addition of a dye. However, only a limited number of dyes are currently available for these labeling strategies.

The most important prerequisite for the dyes used in these labeling strategies is that a sufficient amount of it needs to pass through cellular membrane(s) in order to reach the target protein. To asses the permeability of the cell membrane to the new fluorinated rhodamines, the following protocol was used. The living mammalian cells (PtK2) had been grown overnight on cover slips and then they were subjected to either 500 or 50 μg of a dye in 1 mL of the growth medium for 15 min. (The amount of a dye used for the labeling of SNAP-fusion proteins is below 5 μg in 1 mL.) After that, the cells were washed with a pure growth medium (without a dye) for 15 min and imaged with an epifluorescence microscope (Figure 7).

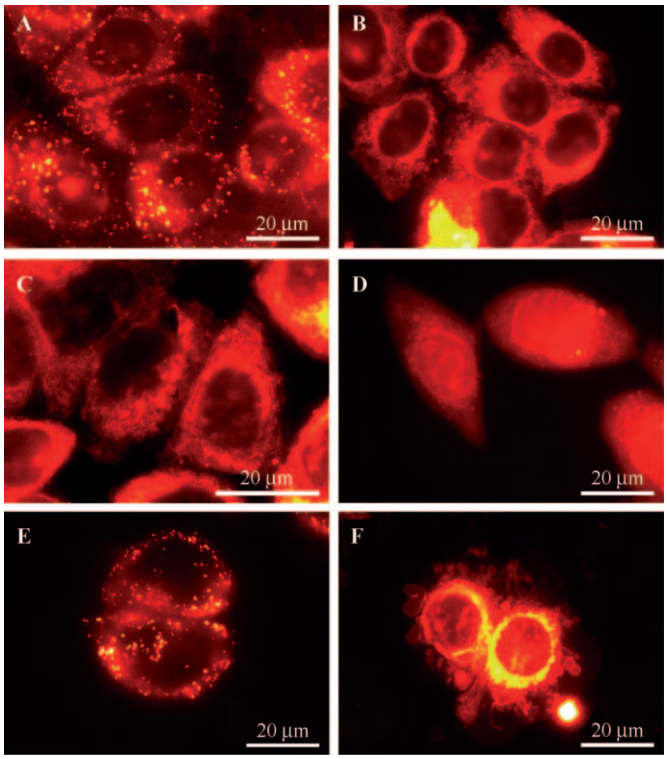

Figure 7. Membrane-permeation experiments of the new rhodamine dyes: Wide-field fluorescence images of living mammalian PtK2 cells after 15-minute incubation with aqueous buffer solution of the dyes. A) **15**-H-CH_2CF_3-H-H (**1g**); B) **1f**-5′-COOH; C) **1f**-5′/6′-COOMe; D) **13**-Me-Me-H (**1q**); E) **1e**-methylester; and F) **9**-H-H (**1i**). The dyes cross the cellular membranes and may thus be used for new labeling strategies in living cells.

Upon treatment with 500 μg of a dye in 1 mL, all the dyes were able to permeate the cellular membrane(s) of living mammalian cells (see Table S2 in the Supporting Information), except two compounds (**15**-H-H-F-5′/6′-COOH (**1d**) and **15**-H-H-F-H (**1c**)). Only 15 min of incubation were enough to non-specifically label intracellular structures like protein aggregates (visible as dots), vesicles or mitochondria. Therefore, this (high) concentration is expected to be sufficient to label proteins specifically, using the labeling strategies based on SNAP-, CLIP- or Halo-tags. The dyes still reached the interior of living cells (Table S3 and Figure 11 in the Supporting Information) upon treatment with 50 μg of a dye in 1 mL of the solution. However, the nonspecifically labeled structures were dimmer, in accordance with the lower concentration of a dye inside the cells. Interestingly, two methyl esters (**1f**-5′/6′-COOMe and **1e**(**14**)-methyl ester) were found among the dyes that penetrate through the cell membrane and stained the organelles even at a lower concentration. This fact indicates that probably the esterification of one or two carboxy groups in rhod-

amines facilitates the ability to cross membranes of live cells.

In summary, the new dyes are able to cross the cellular membrane(s) and reach the interior of living cells. They may be used as an addition to the currently available dyes for the new labeling strategies in living cells (e.g., *N,N,N′,N′*-tetramethylrhodamine).

Conclusion and Outlook

New fluorinated rhodamines serving as excellent fluorescent markers in (live) cell microscopy and nanoscopy were introduced. They can be excited between $\lambda = 470$ to 515 nm with common solid sate or argon ion lasers, have large absorption cross-sections, emit light at about $\lambda = 520$ nm with high fluorescence quantum yields in solution (in a free state and after bioconjugation) and possess relatively long fluorescence lifetimes of 3–4 ns. Their intersystem crossing rates are relatively low and they are extremely photostable, allowing a very long observation time at low excitation intensities and excellent performance at large excitation intensities. Consequently, these rhodamines perform outstanding in single-molecule based microscopies, such as FCS. The compounds are available in a hydrophilic (sulfonated) and a lipophilic form (with the same chromophore) and amino reactive sites may easily be introduced, utilizing specific labeling of bio-molecules, such as proteins and lipids. Further, the compounds can be used in STED nanoscopy delivering a significantly improved spatial resolution of immunostained cellular structures. Live cell applications may be feasible since the new fluorinated rhodamines have been shown to penetrate the cellular membrane.

The analogue of Rhodamine B with four 2,2,2-trifluoroethyl groups would be an interesting extension of the present "dye gallery". It is one of the most lipophilic "green" fluorescent dyes. However, it is hard to predict, whether this rhodamine could be sulfonated.

Acknowledgements

This work was supported by the Leibnitz Prize Fund of the DFG (S. W. H.) and the Max-Planck-Gesellschaft. The authors are grateful to Donald Ouw for the optical measurements. We highly appreciate the assistance of Reinhard Machinek, Dr. Holm Frauendorf, and their co-workers who recorded numerous NMR and mass spectra at the Institut für Organische und Biomolekulare Chemie (Georg-August-Universität Göttingen).

[1] "Fluorophores for Confocal Microscopy: Photophysics and Photochemistry": R. Y. Tsien, L. Ernst, A. Waggoner in *Handbook of Biological Confocal Microscopy*, 3 ed. (Ed.: J. B. Pawley), Springer, New York, **2006**, pp. 338–352.

[2] a) W. E. Moerner, M. Orrit M, *Science* **1999**, *283*, 1670–1676; b) W. P. Ambrose, P. M. Goodwin, J. H. Jett, A. Van Orden, J. H. Werner, R. A. Keller, *Chem. Rev.* **1999**, *99*, 2929–2956; c) X. S. Xie, J. K. Trautman, *Annu Rev. Phys. Chem.* **1998**, *49*, 441–480; d) W. E. Moerner, *Proc. Natl. Acad. Sci. USA* **2007**, *104*, 12596–12602; e) C. Joo, H. Balci, Y. Ishitsuka, C. Buranachai, T. Ha, *Annu. Rev. Biochem.* **2008**, *77*, 51–76.

[3] For reviews, see: a) S. W. Hell, *Science* **2007**, *316*, 1153–1158; b) M. Fernández-Suárez, A. Y. Ting, *Nat. Rev. Mol. Cell Biol.* **2008**, *9*, 929–943; c) D. Evanko, *Nat. Methods* **2009**, *6*, 19–20; d) S. W. Hell, *Nat. Methods* **2009**, *6*, 24–32; e) X. Zhuang, *Nat. Photonics* **2009**, *3*, 365–367; f) J. Lippincott-Schwartz, S. Manley, *Nat. Methods* **2009**, *6*, 21–23; g) B. Huang, M. Bates, X. Zhuang, *Annu. Rev. Biochem.* **2009**, *78*, 993–1016; for recent reports, see: h) J. A. Fitzpatrick, Q. Yan, J. J. Sieber, M. Dyba, U. Schwarz, C. Szent-Gyorgyi, C. A. Woolford, P. B. Berget, A. S. Waggoner, M. P. Bruchez, *Bioconjugate Chem.* **2009**, *20*, 1843–1847; i) E. Betzig, G. H. Patterson, R. Sougrat, O. W. Lindwasser, S. Olenych, J. S. Bonifacino, M. W. Davidson, J. Lippincott-Schwartz, H. F. Hess, *Science* **2006**, *313*, 1642–1645; j) M. J. Rust, M. Bates, X. Zhuang, *Nat. Methods* **2006**, *3*, 793–795; k) M. Bates, B. Huang, G. T. Dempsey, X. Zhuang, *Science* **2007**, *317*, 1749–1753; l) S. T. Hess, T. P. K. Girirajan, M. D. Mason, *Biophys. J.* **2006**, *91*, 4258–4272; m) J. Fölling, V. Belov, R. Kunetsky, R. Medda, A. Schönle, A. Egner, C. Eggeling, M. Bossi, S. W. Hell, *Angew. Chem.* **2007**, *119*, 6382–6386; *Angew. Chem. Int. Ed.* **2007**, *46*, 6266–6270; n) J. Fölling, V. Belov, D. Riedel, A. Schönle, A. Egner, C. Eggeling, M. Bossi, S. W. Hell, *ChemPhysChem* **2008**, *9*, 321–326; o) M. Bossi, J. Fölling, V. N. Belov, V. P. Boyarskiy, R. Medda, A. Egner, C. Eggeling, A. Schönle, S. W. Hell, *Nano Lett.* **2008**, *8*, 2463–2468; p) V. P. Boyarskiy, V. N. Belov, R. Medda, B. Hein, M. Bossi, S. W. Hell, *Chem. Eur. J.* **2008**, *14*, 1784–1792; q) S. M. Polyakova, V. N. Belov, C. Eggeling, S. F. Yan, C. Ringemann, G. Schwarzmann, A. de Meijere, S. W. Hell, *Eur. J. Org. Chem.* **2009**, 5162–5177; r) V. N. Belov, M. L. Bossi, J. Fölling, V. P. Boyarskiy, S. W. Hell, *Chem. Eur. J.* **2009**, *15*, 10762–10776; s) H. Shroff, C. G. Galbraith, J. A. Galbraith, H. White, J. Gilette, S. Olenych, M. W. Davidson, E. Betzig, *Proc. Natl. Acad. Sci. USA* **2007**, *104*, 20308–20313; t) B. Huang, W. Wang, M. Bates, X. Zhuang, *Science* **2008**, *319*, 810–813; u) B. Huang, S. A. Jones, B. Brandenburg, X. Zhuang, *Nat. Methods* **2008**, *5*, 1047–1052.

[4] a) D. Magde, E. Elson, W. W. Webb, *Phys. Rev. Lett.* **1972**, *29*, 705–708; b) M. Ehrenberg, R. Rigler, *Chem. Phys.* **1974**, *4*, 390–401; c) E. Hausteinand, P. Schwille, *Methods* **2003**, *29*, 153–166.

[5] Y. Chen, J. D. Müller, P. T. C. So, E. Gratton, *Biophys. J.* **1999**, *77*, 553–567; P. Kask, K. Palo, D. Ullmann, K. Gall, *Proc. Natl. Acad. Sci. USA* **1999**, *96*, 13756–13761.

[6] C. Eggeling, L. Brand, D. Ullmann, S. Jaeger, *Drug Discovery Today* **2003**, *8*, 632–641.

[7] C. Eggeling, J. Widengren, R. Rigler, C. A. M. Seidel, *Anal. Chem.* **1998**, *70*, 2651–2659.

[8] a) S. W. Hell, J. Wichmann, *Opt. Lett.* **1994**, *19*, 780–782; b) T. A. Klar, S. Jakobs, M. Dyba, A. Egner, S. W. Hell, *Proc. Natl. Acad. Sci. USA* **2000**, *97*, 8206–8210.

[9] a) M. Dyba, S. W. Hell, *Appl. Opt.* **2003**, *42*, 5123–5129; b) G. Donnert, J. Keller, R. Medda, M. A. Andrei, S. O. Rizzoli, R. Lührmann, R. Jahn, C. Eggeling, S. W. Hell, *Proc. Natl. Acad. Sci. USA* **2006**, *103*, 11440–11445.

[10] For a general description and spectral range of rhodamines as fluorescent dyes, see: a) M. Beija, C. A. M. Afonso, J. M. G. Martinho, *Chem. Soc. Rev.* **2009**, *38*, 2410–2433; M. S. T. Gonçalves, *Chem. Rev.* **2009**, *109*, 190–212; b) R. P. Haugland, *A Guide to Fluorescent Probes and Labeling Technologies*, Invitrogen, Carlsbad, **2005**, pp. 11–37; c) for the use of rhodamines in bioconjugation techniques, see: G. T. Hermanson, *Bioconjugate Techniques*, Academic Press, Amsterdam, **2008**, pp. 415–427; for laser dyes' properties of rhodamines, see: d) F. P. Schäfer in *Dye Lasers* (Ed.: F. P. Schäfer), Springer, Berlin, **1990**, pp. 3–4; e) K.-H. Drexhage in *Dye Lasers* (Ed.: F. P. Schäfer), Springer, Berlin, **1990**, p. 158; f) K.-H. Drexhage in *Dye Lasers* (Ed.: F. P. Schäfer), Springer, Berlin, **1990**, p. 175–180; g) K.-H. Drexhage, *Top. Appl. Phys.* **1973**, *1*, 155–200; for the most recent report on the new red-emitting rhodamines, see: h) K. Kolmakov, V. N. Belov, J. Bierwagen, C. Ringemann, V. Müller, C. Eggeling, S. W. Hell, *Chem. Eur. J.* **2010**, *16*, 158–166.

[11] a) K. Peneva, G. Mihov, F. Nolde, S. Rocha, J. Hotta, K. Braeckmans, J. Hofkens, H. Uji-i, A. Hermann, K. Müllen, *Angew. Chem.* **2008**, *120*, 3420–3423; *Angew. Chem. Int. Ed.* **2008**, *47*, 3372–3375; b) C. Jung, B. K. Müller, D. C. Lamb, F. Nolde, K. Müllen, C. Bräuchle, *J. Am. Chem. Soc.* **2006**, *128*, 5283–5291.
[12] Z. Lu, N. Liu, S. J. Lord, S. D. Bunge, W. E. Moerner, R. J. Twieg, *Chem. Mater.* **2009**, *21*, 797–810.
[13] a) G. Ulrich, R. Ziessel, A. Harriman, *Angew. Chem.* **2008**, *120*, 1202–1219; *Angew. Chem. Int. Ed.* **2008**, *47*, 1184–1201. For a very recent report on the hydrophilic BODIPY fluorophores decorated with sulfonic acid residues, see: b) S. L. Niu, G. Ulrich, R. Ziessel, A. Kiss, P.-Y. Renard, A. Romieu, *Org. Lett.* **2009**, *11*, 2049–2052.
[14] F. Mao, W.-Y. Leung, R. P. Haugland (Molecular Probes), US Patent 6130101, **2000**.
[15] This conclusion follows from the comparison of the stabilities of the Oregon Green dyes—fluorescein derivatives bearing two fluorine atoms at the positions 2′ and 7′ of the xanthene ring—with that of the parent dye; see the Supporting Information for the details.
[16] S. W. Hell, V. N. Belov, G. Mitronova, M. Bossi, G. Moneron, C. A. Wurm, S. Jakobs, C. Eggeling, J. Bierwagen, L. Meyer (Max-Planck-Gesellschaft zur Förderung der Wissenschaften e.V.), PCT/EP 2009/004650, **2009**.
[17] K. R. Gee, M. Poot, D. H. Klaubert, W.-C. Sun, R. P. Haugland, F. Mao (Molecular Probes), WO97/39064, **1997**.
[18] The "hybrid" of Rhodamine B ($\lambda_{abs.}=545$, $\lambda_{em.}=569$ nm, $\varepsilon=114000$, $\Phi_{fl}=52\,\%$) and fluoresceine ($\lambda_{abs.}=497$ $\lambda_{em.}=518$ nm, $\varepsilon=84000$, $\Phi_{fl}=100\,\%$) was reported to absorb at $\lambda=517$ nm and emit at $\lambda=542$ nm ($\varepsilon=39000$, $\Phi_{fl}=58\,\%$): P. R. Hammond, *J. Photochem.* **1979**, *10*, 467–471.
[19] P. R. Hammond, J. F. Feeman (US Dep. Energy), US Patent 4945176, **1989**; P. R. Hammond, J. F. Feeman (US Dep. Energy), US Patent 5047559, **1991**; P. R. Hammond, J. F. Feeman (US Dep. Energy), US Patent 5111472, **1991**.
[20] S. Bigotti, A. Volonterio, M. Zanda, *Synlett* **2008**, 958–962.
[21] For the structure of Rhodamine 110 and other similar and commercially available "green" fluorescent dyes, see Figure 1S in the Supporting Information.
[22] R. F. Kubin, A. N. Fletcher, *J. Lumin.* **1982**, *27*, 455–462.
[23] To prevent the formation of the cyclic non-fluorescent amides formed from the sterically hindered carboxy group of the mono-carboxy rhodamines and primary amines, an additional linker with a secondary amide group should be introduced to this carboxy group; for an example, see reference [3p].
[24] T. Cohen, A. G. Dietz, Jr., J. Miser, *J. Org. Chem.* **1977**, *42*, 2053–2058.
[25] C. Eggeling, J. Widengren, R. Rigler, C. A. M. Seidel in *Applied Fluorescence in Chemistry, Biology and Medicine* (Eds.: W. Rettig, B. Strehmel, M. Schrader, H. Seifert), Springer, Berlin, **1999**, p. 193.
[26] For a short review on the photobleaching kinetics of Rhodamine 6G, see: a) C. Eggeling, A. Volkmer, C. A. M. Seidel, *ChemPhysChem* **2005**, *6*, 791–804 and the references therein; b) V. E. Korobov, A. K. Chibisov, *J. Photochem.* **1978**, *9*, 411–424; c) radicals, which were formed by irradiation of Rhodamine 6G in solution, were detected by ESR spectroscopy: R. Zondervan, F. Kulzer, S. B. Orlinskii, M. Orrit, *J. Phys. Chem. A* **2003**, *107*, 6770–6776.
[27] M. Kasha, *Rad. Res.* **1960**, *2*, 243–275.
[28] a) A. K. Chibisov, H. Görner, *J. Photochem. Photobiol. A* **1997**, *105*, 261–267; b) G. Donnert, C. Eggeling, S. W. Hell, *Nat. Methods* **2007**, *4*, 81–86.
[29] a) M. Anbar, E. J. Hart, *J. Am. Chem. Soc.* **1964**, *86*, 5633–6537; b) E. V. Khoroshilova, D. N. Nikogosyan, *J. Photochem. Photobiol. B* **1990**, *5*, 413–427.
[30] a) J. Widengren, U. Mets, R. Rigler, *J. of Phys. Chem.* **1995**, *99*, 13368–13379; b) J. Widengren, R. Rigler, *Bioimaging* **1996**, *4*, 149–157; c) P. S. Dittrich, P. Schwille, *Appl. Phys. B* **2001**, *73*, 829–837.
[31] C. Ringemann, A. Schönle, A. Giske, C. von Middendorff, S. W. Hell, C. Eggeling, *ChemPhysChem* **2008**, *9*, 612–624.
[32] K. I. Willig, B. Harke, R. Medda, S. W. Hell, *Nat. Methods* **2007**, *4*, 915–918.
[33] a) K. Simons, E. Ikonen, *Nature* **1997**, *387*, 569–572; b) *Lipid Rafts and Caveolae* (Ed.: C. J. Fielding), Wiley-VCH, Weinheim, **2006**; c) K. Jacobson, O. G. Mouritsen, R. G. W. Anderson, *Nat. Cell Biol.* **2007**, *9*, 7–14; d) M. F. Hanzal-Bayer, J. F. Hancock, *FEBS Lett.* **2007**, *581*, 2098–2104.
[34] C. Eggeling, C. Ringemann, R. Medda, G. Schwarzmann, K. Sandhoff, S. Polyakova, V. N. Belov, B. Hein, C. von Middendorff, A. Schönle, S. W. Hell, *Nature* **2009**, *457*, 1159–1163.
[35] a) H. M. O'Hare, K. Johnsson, A. Gautier, *Curr. Opin. Struct. Biol.* **2007**, *17*, 488–494; b) T. Gronemeyer, G. Godin, K. Johnsson, *Curr. Opin. Biotechnol.* **2005**, *16*, 453–458.

Received: November 30, 2009

Please note: Minor changes have been made to this publication in *Chemistry–A European Journal* Early View. The Editor.

Published online: March 22, 2010

